

Isolated Majorana mode in a quantum computer from a duality twist

Sutapa Samanta,¹ Derek S. Wang,² Armin Rahmani,^{1,3} and Aditi Mitra⁴

¹*Department of Physics and Astronomy, Western Washington University, Bellingham, Washington 98225, USA*

²*IBM Quantum, IBM T.J. Watson Research Center, Yorktown Heights, New York 10598, USA*

³*Advanced Materials Science and Engineering Center,
Western Washington University, Bellingham, Washington 98225, USA*

⁴*Center for Quantum Phenomena, Department of Physics,
New York University, 726 Broadway, New York, New York 10003, USA*

Investigating the interplay of dualities, generalized symmetries, and topological defects beyond theoretical models is an important challenge in condensed matter physics and quantum materials. A simple model exhibiting this physics is the transverse-field Ising model, which can host a noninvertible topological defect that performs the Kramers-Wannier duality transformation. When acting on one point in space, this duality defect imposes the duality twisted boundary condition and binds a single Majorana zero mode. This Majorana zero mode is unusual as it lacks localized partners and has an infinite lifetime, even in finite systems. Using Floquet driving of a closed Ising chain with a duality defect, we generate this Majorana zero mode in a digital quantum computer. We detect the mode by measuring its associated persistent autocorrelation function using an efficient sampling protocol and a compound strategy for error mitigation. We also show that the Majorana zero mode resides at the domain wall between two regions related by a Kramers-Wannier duality. Finally, we highlight the robustness of the isolated Majorana zero mode to integrability and symmetry-breaking perturbations. Our findings offer an approach to investigating exotic topological defects in digitized quantum devices.

Introduction.— Symmetry is a cornerstone of modern physics. Traditionally, symmetries in quantum systems are realized as unitary representations of a group of transformations that leave the Hamiltonian invariant. Dualities are transformations that relate two different theories, or different phases of the same theory, and are closely related to symmetry but cannot always be described within the traditional framework [1–4]. This is because they can act as projectors; therefore, they do not admit a unitary representation but are examples of noninvertible symmetries [5–9]. Both unitary (invertible) and noninvertible symmetries are described within the recently developed framework of *generalized symmetries* [10, 11], and can manifest through topological defects [7, 9, 12, 13].

Understanding the role of topological defects, both of the invertible and noninvertible kind, is one of the forefronts of condensed-matter and high-energy physics [14, 15]. Despite remarkable theoretical progress, detecting exotic topological defects associated with generalized symmetries is challenging in traditional condensed-matter systems, rendering their experimental realization an open question. Here, for the first time, we realize such a system on a synthetic platform, a small, noisy quantum computer [16].

The Kramers-Wannier duality transformation of the transverse-field Ising model (TFIM) is one of the most well-known dualities [17]. The TFIM can host topological defects, one of them being the duality defect [7, 9, 18] and the other the familiar unitary spin-flip defect that captures the Z_2 symmetry of the model. The duality defect is one of the simplest examples of a noninvertible transformation as it projects out states of a given

Z_2 symmetry [7]. A duality defect acting at a particular point in space imposes a special “twisted” boundary condition [19–23]. One of the consequences of the duality twist defect is the emergence of a Majorana zero mode with distinct characteristics from other Majorana modes occurring in the TFIM.

It is well known that the TFIM with open boundary conditions can host Majorana edge modes [24, 25] in the topological phase, both in equilibrium and in its Floquet versions [26, 27]. These edge modes appear in pairs, and have a lifetime which grows exponentially with the system size because they can hybridize by tunneling. On the other hand, the Majorana appearing due to a duality twist defect is isolated, lacking a localized partner. It thus has an infinite lifetime, even in finite systems. In addition, this isolated mode exists for all couplings of the static and Floquet versions of the TFIM, and splits the chain into two parts whose couplings are related by the Kramers-Wannier duality transformation [7, 28]. Digitized quantum devices have provided a new playground for realizing topological physics [29–36]. In particular, Floquet versions of the TFIM with open boundary conditions have been studied on current noisy quantum devices [35, 37]. Here we probe the Floquet version of the TFIM with a duality twist defect.

In this paper, we implement the duality twist defect in a closed chain of 20 qubits on the `ibmq_kolkata` device and observe an isolated Majorana zero mode. By obtaining the autocorrelation functions of several operators in the quantum device, we demonstrate that the Majorana zero mode, with a theoretically infinite lifetime, is persistent. We also verify that weak perturbations that break both integrability and the Z_2 symmetry

of the problem do not destabilize the zero mode for chains of finite length. We further explore the properties of this mode by applying a circuit that moves the twist defect, observing that, surprisingly, the Majorana does not follow the defect but stays in its original position. This observation demonstrates that the twist defect is topological, so its translations do not modify the physics.

Unpaired Majorana in the Floquet-TFIM with a duality twist.— We consider the one dimensional TFIM with L sites, whose Hamiltonian is given by $H = J \sum_{j=0}^{L-1} \sigma_j^z \sigma_{j+1}^z + g \sum_{j=0}^{L-1} \sigma_j^x$. The system has no open ends, and periodic boundary conditions are imposed where the operator at site $L+j$ is identified with the operator at site j . Duality-twisted boundary conditions are implemented by applying a twist on the $r, r-1$ sites which changes $\sigma_{r-1}^z \sigma_r^z$ to $\sigma_{r-1}^z \sigma_r^x$, and removes the transverse field $g \sigma_r^x$, on that site [7]. Then the twisted Hamiltonian becomes

$$H_t = H_{zz} + H_{zx} + H_x, \quad (1)$$

where

$$H_{zz} = J \sum_{j \neq r-1} \sigma_j^z \sigma_{j+1}^z, \quad H_{zx} = J \sigma_{r-1}^z \sigma_r^x, \quad H_x = g \sum_{j \neq r} \sigma_j^x.$$

There is nothing special about the sites $r, r-1$, and a local unitary transformation can move the twist defect from one pair of sites to the neighboring pair of sites [7, 28, 38].

The Floquet unitary operator for the twisted model can be written as [18]

$$U = e^{-iH_x/2} e^{-iH_{zx}/2} e^{-iH_{zz}/2}. \quad (2)$$

Importantly, the presence of the duality twist modifies the Z_2 symmetry from $\mathcal{D}_\psi = \prod_{j=0}^{L-1} \sigma_j^x$ to $\Omega_r = i \sigma_r^z \mathcal{D}_\psi$. The above model, in a given Z_2 sector, is quadratic in Majorana fermions, and hence integrable (exactly solvable). The analytic expression of the duality-twist Majorana zero mode for the above Floquet set-up was derived in [18, 28]. Similar to Majorana edge modes with open boundary conditions, the Majorana zero mode with a duality twist is a sum involving Majoranas all along the chain. For the Majorana mode with the duality twist, the largest weight is in the vicinity of site r , while the Majorana pairs with open boundary conditions have their largest weight at the boundaries.

The Majorana zero mode with a duality twist has important differences with the Majorana pairs that appear for open boundary conditions. While the latter occurs only in the topological phase $J > g$, the Majorana zero mode with the duality twist occurs for all values of g, J , including $g > J, g < J$ and even disordered ones. Only its localization length is determined by the strength of the disorder and average values of g and J . There is a simple counting argument for this. If one writes the model in

terms of Majorana fermions, there are $2L$ Majoranas in the Hilbert space for a chain of L sites. The twist results in a unitary with $2L - 1$ Majoranas. Since the determinant of the orthogonal matrix that evolves the Majoranas has to be 1, it forces an odd number of eigenvalues of 1, where the corresponding eigenvectors are the Majorana zero modes.

Since the Majorana with the duality twist lacks a partner, it never decays in time, i.e., it has an infinite lifetime rather than a lifetime that is exponential in the system size. The mathematical reason for this is that the Majorana zero mode with the duality twist is a symmetry of the system as it commutes both with the generator of time-evolution as well as the Z_2 symmetry Ω_r . In contrast, the Majorana pairs with open boundary conditions anticommute with the associated Z_2 symmetry \mathcal{D}_ψ .

In the spin representation, the Majorana at site r is identical to the Pauli operator σ_r^y [18, 28]. (In the figures, we denote $\sigma_i^{x,y,z}$ with X_i, Y_i, Z_i for notational brevity.) In addition, the farther away a Majorana is from r , the longer is the corresponding Pauli string. To detect the Majorana zero mode, we employ the infinite temperature autocorrelation function, defined as

$$A_{\mathcal{O}}(n) = \frac{1}{2^L} \text{Tr} \left[\mathcal{O}(n) \mathcal{O} \right], \quad (3)$$

of an operator \mathcal{O} , where the Heisenberg operator after n Floquet steps is given by $\mathcal{O}(n) = (U^\dagger)^n \mathcal{O} U^n$. The signature of the zero mode is the temporal persistence of a non-zero autocorrelation function for σ_r^y . In contrast, the autocorrelation function of other operators, with no overlap with a conserved quantity, are expected to decay to zero due to dephasing.

To measure the autocorrelation function, we represent the trace as a sum of expectation values $\langle k | \mathcal{O}(n) \mathcal{O} | k \rangle$ in a basis chosen to be the eigenbasis of \mathcal{O} , $\mathcal{O} | k \rangle = \lambda_k | k \rangle$. Each expectation value in the trace can then be measured by measuring $\langle \mathcal{O}(n) \rangle$ at time n after applying the Floquet circuit to the initial state $| k \rangle$. For operators \mathcal{O} corresponding to Pauli operators (or Pauli strings), the states $| k \rangle$ can be chosen to be easy-to-prepare direct products of single-qubit states. The detection of the trace can nevertheless seem challenging because we have an exponentially large number of basis states $| k \rangle$. However, a random sampling of a small number of basis states and performing a partial sum yield accurate approximations to the trace (3), as discussed in the Supplemental Material.

Detection of the unpaired Majorana in the IBM quantum device— We have chosen the values of the coupling constants to be $J = 0.75\pi$ and $g = 0.2\pi$ for all the computations in this paper, although similar results can be obtained for other coupling constants. To create and detect the zero mode in the quantum computer, we apply a quantum circuit that generates the

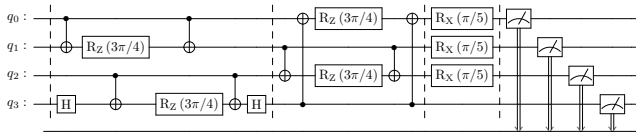


FIG. 1. Implementation of the unitary (2) for a 4-qubit system in a quantum computer. The duality twist corresponds to modifying the Floquet TFIM by removing the transverse field on qubit 3 and applying a twist exchange interaction $\sigma_2^z \sigma_3^z$ between qubits 2 and 3. Periodic boundary conditions have been imposed with a $\sigma_3^z \sigma_0^z$ exchange interaction.

Floquet dynamics by the repeated applications of a circuit block corresponding to the unitary operator in (2). A simple 4-qubit version of this block, corresponding to one Trotter step, is shown in Fig. 1. We compute the autocorrelation (3) for $\mathcal{O} = \sigma^x, \sigma^y$, and σ^z of a 20-qubit system. We perform this calculation on the 27-qubit `ibmq_kolkata` device with a 20-qubit closed loop. Thus, the device geometry eliminates the need for using swap gates to implement periodic boundary conditions. We used a compound error mitigation method as discussed in the Supplemental Material and described in Refs. [36, 39].

As mentioned above, for a Pauli operator \mathcal{O} , we need to create initial states that are eigenstates of the corresponding Pauli operator. Measuring $\mathcal{O} = \sigma^z$ is the simplest as the input and output in IBM devices are measured in the eigenbasis of σ^z by default. However, both initialization and measurement in a different basis can be implemented through rotation operators $R_y(\pi/2)$ ($R_x(-\pi/2)$) that rotate from the z to the x (y) direction.

In Fig. 2, we present both simulation and quantum-hardware results for the bulk and defect autocorrelation functions obtained from the partial trace with 20 random basis states. We also show simulation results from Qiskit Aer simulators for 12-qubit and 20-qubit systems. The simulation results exhibit very small system-size dependence, indicating that the 20-qubit system accurately captures the thermodynamic limit. Furthermore, the results from the `ibmq_kolkata` device for the 20-qubit system is in good agreement with the simulations. We observe that the autocorrelation function of $\mathcal{O} = \sigma_r^y$ at the twist defect $r = L - 1$ does not decay, which overlaps with the emergent Majorana zero mode. In contrast, all other autocorrelators decay to zero in the long time limit. The persistence of the autocorrelation function of the operator corresponding to the unpaired Majorana, during the Floquet dynamics, provides evidence for the dynamical generation of this mode in a digitized quantum device.

Unitary translation of twist defect— A hallmark of a topological defect is that it can be moved by local unitary transformations. Here the word “topological” is used in the following sense: if we think of the 1+1 dimensional system as a torus, then the twist defect is a

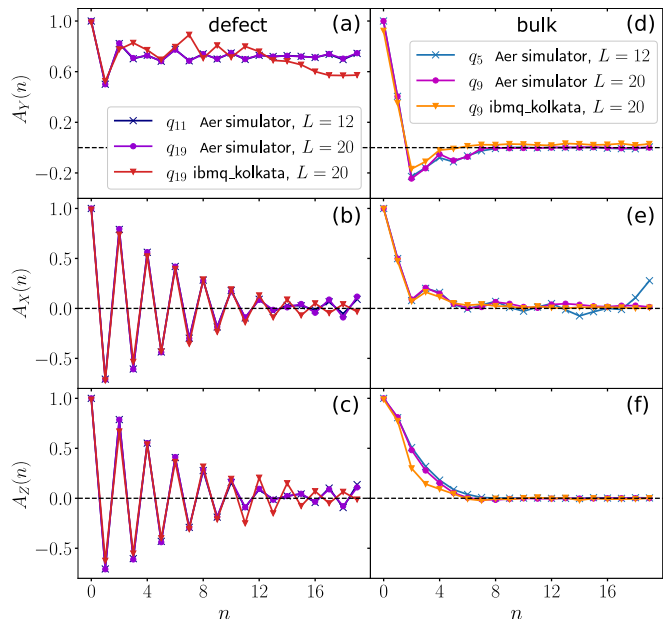


FIG. 2. Signature of Majorana zero mode at the defect site for duality-twisted Floquet-TFIM. Panel (a) shows the non-decaying autocorrelation for σ_y at the defect site $r = L - 1$, which overlaps with the zero mode. All other autocorrelations both at the twist defect $r = L - 1$ [panel (b), (c)] and at a bulk site $j = -1 + L/2$ [panel (d), (e), (f)], far away from the twist defect, decay with time. The chosen bulk qubit behaves qualitatively similarly to other bulk qubits. We present data from `ibmq_kolkata` device for $L = 20$, the longest physical loop of qubits available in the device. There is good qualitative agreement between simulation and measurements on the quantum device. The simulations were also performed for a smaller system of 12 qubits. The agreement between the two system sizes $L = 12, 20$ indicates that we are capturing the behavior in the thermodynamic limit.

line that spans the time direction. In Euclidean time and with periodic boundary conditions, the twist defect has a winding number of 1, and the partition function is invariant to local deformations of the defect. In particular, a unitary transformation of the form $U_r = CZ_{r-1,r} H_{r-1}$, where $CZ_{r-1,r}$ is a controlled-Z gate, and H_{r-1} is a Hadamard gate, moves the twist-defect from the sites $(r - 1, r)$ to sites $(r - 2, r - 1)$ [7, 28]. Fig. 3 illustrates this for a 4-qubit system. The unitary U_r introduces a transverse field at site r of strength J while eliminating the transverse field at site $r - 1$. It also changes the terms $J\sigma_{r-2}^z \sigma_{r-1}^z$ and $J\sigma_{r-1}^z \sigma_r^x$ to $J\sigma_{r-2}^z \sigma_{r-1}^x$ and $g\sigma_{r-1}^z \sigma_r^z$. Thus a Kramers-Wannier duality transformation has been performed on the sites $r, r - 1$ where the roles of g, J have been interchanged. Remarkably, the Majorana zero mode stays localized at r , and now separates two regions of the chain that are related by the Kramers-Wannier duality transformation. Although the Majorana zero mode stays localized at site r , in the language of Pauli strings, it is a more nonlocal object. In particular, instead of having an overlap with σ_r^y , it now

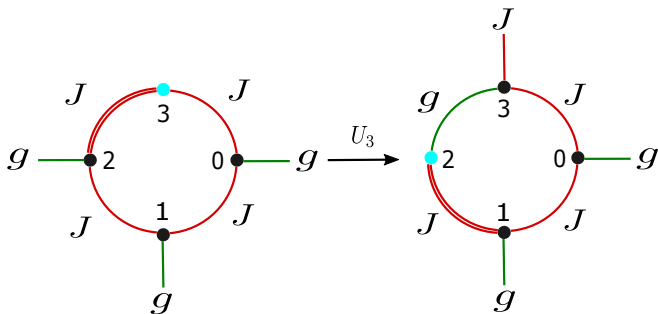


FIG. 3. A twist defect that was originally on sites 2 and 3 (left) is moved to sites 1 and 2 (right) by a unitary transformation $CZ_{2,3}H_2$. Cyan denotes the site r at which there is no magnetic field while the double red lines denote a twist interaction $\sigma_{r-1}^z \sigma_r^x$. Vertical lines between sites $j, j+1$ denote a $\sigma_j^z \sigma_{j+1}^z$ interaction. After the unitary transformation (right), note the Kramers-Wannier duality between sites 2,3 and the rest of the chain where the strength of the transverse field at site 3 is J while the exchange interaction between qubits 2 and 3 is g . The unitary transformation shifts the twist but not the Majorana zero mode which stays localized at site 3. Thus the Majorana zero mode resides at the domain wall across which g, J exchange roles.

has an overlap with $\sigma_{r-1}^x \sigma_r^y$.

The Majorana zero mode after a translation of the twist defect from (18, 19) to (17, 18) for a 20-qubit system is shown in Fig. 4. After one translation, the Majorana is still localized at site $r = 19$, but in the language of Pauli spins, this Majorana zero mode no longer has an overlap with σ_{19}^y , but rather with the longer string $\sigma_{18}^x \sigma_{19}^y$.

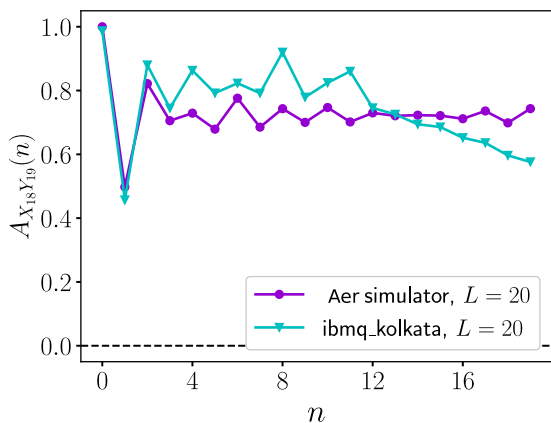


FIG. 4. Unpaired Majorana in the `ibmq_kolkata` device for $L = 20$ after a unitary translation that has moved the twist defect from sites 18, 19 to sites 17, 18. The Majorana stays localized at site 19 but now has an overlap with the longer Pauli string $\sigma_{18}^x \sigma_{19}^y$.

Effects of Interactions— Now we add perturba-

tions to the model (1) through the term

$$H_{xx} = J_x \sum_j \sigma_j^x \sigma_{j+1}^x. \quad (4)$$

In the language of Majorana fermions, the above is a four-fermion and hence interacting term. The Floquet unitary is now given by

$$U_{\text{int}} = e^{-iH_{xx}/2} e^{-iH_x/2} e^{-iH_{zx}/2} e^{-iH_{zz}/2}. \quad (5)$$

Note that H_{xx} not only breaks integrability, but it also does not commute with the discrete symmetry Ω_r due to the $\sigma_{r\pm 1}^x \sigma_r^x$ terms. We repeat the same quantum simulation for the interacting model with the defect location at site $r = L - 1$. We find that the σ_r^y -correlator at the defect remains constant, while all other correlators decay with time (see Fig. 2 of the Supplemental Material). However, the full dynamics of the σ_r^y -correlator at the defect is not captured in this figure as we can run the Floquet dynamics in the device only for a short time, about 20 Floquet cycles, before noise takes over. We show the theoretical behavior of the Majorana zero mode by performing exact diagonalization for long times in Fig. 5(a). The Majorana modes decay to a plateau, and the plateau height decreases with increasing interactions J_x . We capture only the initial portions of this behavior in the quantum device (see Fig. 5(b) and (c)).

Conclusions.— In this paper, we investigate the physics of the duality twist defect and the corresponding emergent Majorana zero mode in a periodically driven TFIM loop of 20 qubits on the IBM superconducting quantum device. The interplay of topological effects and symmetries can lead to novel phenomena. The Majorana zero mode generated by a duality twist in a TFIM chain commutes with the Z_2 charge of the model and thus, theoretically, has an infinite lifetime in finite systems [18] (in contrast to Majorana edge states with open boundary conditions that are vulnerable to exponential hybridization). Using efficient random sampling, we obtained an accurate approximation to various autocorrelation functions and provided evidence, on the quantum computer, for the emergence of the unpaired Majorana mode bound to the duality twist defect. Furthermore, we explored the effects of moving the duality twist defect with unitary gates, and the effect of integrability and symmetry-breaking perturbations. This work opens a new avenue for physically creating and investigating novel topological defects in quantum systems. Future improvements in hardware quality and error mitigation may allow accessing longer evolution times with deeper circuits, providing access to the long-time plateaus of persistent autocorrelation functions in the presence of interactions. Exciting directions of future research include implementing topological defects on the quantum computer, not only in Z_n spin chains [9], but also in two-dimensional Floquet codes [40].

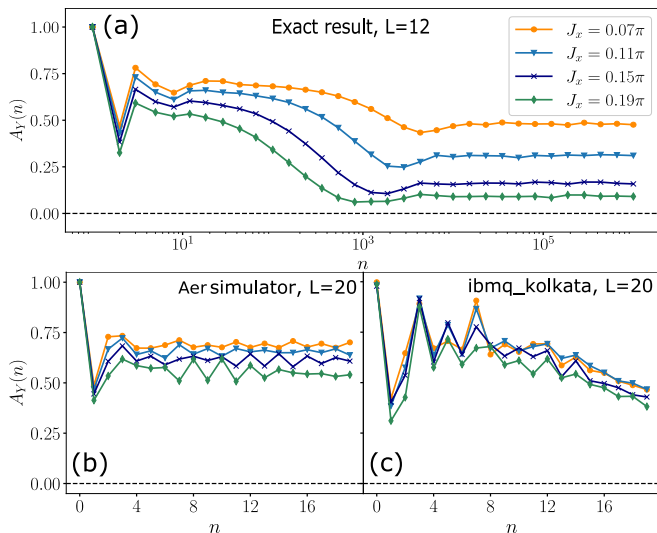


FIG. 5. Stability of the Majorana zero mode to integrability- and symmetry-breaking perturbations in a finite system. The autocorrelation function of σ_r^y at the defect $r = L - 1$, for different values of the perturbation J_x , are presented. Panel (a) shows the numerical results for system size $L = 12$ up to large Floquet time steps. The autocorrelation stabilizes at a nonzero plateau, which is a finite size effect (the plateau height vanishes as $L \rightarrow \infty$ [28]). While we are not able to access the plateau in the long-time limit in the `ibmq_kolkata` device due to noise, panels (b) and (c) show results from the IBM simulator and the `ibmq_kolkata` device, respectively, for intermediate timescales, indicating the persistence of the autocorrelation function up to these accessible timescales.

Acknowledgements: We thank Oles Shtanko for helpful comments and discussions. We acknowledge the use of IBM Quantum services. We also thank the Brookhaven National Laboratory for providing access to IBM devices. This work was supported by the US National Science Foundation under Grants NSF DMR-2018358 (AM) and DMR-1945395 (AR and SS), and in part by the US National Science Foundation under Grant No. NSF PHY-1748958 (AR and AM).

[1] E. Cobanera, G. Ortiz, and Z. Nussinov, The bond-algebraic approach to dualities, *Adv. Phys.* **60**, 679 (2011).
 [2] N. Seiberg, T. Senthil, C. Wang, and E. Witten, A duality web in 2+1 dimensions and condensed matter physics, *Ann. Phys.* **374**, 395 (2016).
 [3] A. M. Somoza, P. Serna, and A. Nahum, Self-dual criticality in three-dimensional z_2 gauge theory with matter, *Phys. Rev. X* **11**, 041008 (2021).
 [4] L. Lootens, C. Delcamp, G. Ortiz, and F. Verstraete, Dualities in one-dimensional quantum lattice models: symmetric hamiltonians and matrix product operator intertwiners, arXiv:2112.09091 (2021).
 [5] E. Verlinde, Fusion rules and modular transformations in

2d conformal field theory, *Nucl. Phys. B* **300**, 360 (1988).
 [6] L. Bhardwaj, L. E. Bottini, S. Schäfer-Nameki, and A. Tiwari, Non-invertible higher-categorical symmetries, *SciPost Phys.* **14**, 007 (2023).
 [7] D. Aasen, R. S. K. Mong, and P. Fendley, Topological defects on the lattice: I. the ising model, *J. Phys. A: Math. Theor.* **49**, 354001 (2016).
 [8] R. Thorngren and Y. Wang, Fusion category symmetry i: Anomaly in-flow and gapped phases, arXiv:1912.02817 (2019).
 [9] D. Aasen, P. Fendley, and R. S. Mong, Topological defects on the lattice: dualities and degeneracies, arXiv:2008.08598 (2020).
 [10] L. Kong, T. Lan, X.-G. Wen, Z.-H. Zhang, and H. Zheng, Algebraic higher symmetry and categorical symmetry: A holographic and entanglement view of symmetry, *Phys. Rev. Res.* **2**, 043086 (2020).
 [11] J. McGreevy, Generalized Symmetries in Condensed Matter, arXiv:2204.03045 (2022).
 [12] D. Gaiotto, A. Kapustin, N. Seiberg, and B. Willett, Generalized global symmetries, *J. High Energy Phys.* **2015** (2), 172.
 [13] D. Gaiotto, J. H. Lee, and J. Wu, Integrable kondo problems, *J. High Energy Phys.* **2021** (4).
 [14] M. Cheng and N. Seiberg, Lieb-schultz-mattis, luttinger, and 't hooft – anomaly matching in lattice systems, arXiv:2211.12543 (2023).
 [15] L. Eck and P. Fendley, From the xxz chain to the integrable rydberg-blockade ladder via non-invertible duality defects, arXiv:2302.14081 (2023).
 [16] J. Preskill, Quantum Computing in the NISQ era and beyond, *Quantum* **2**, 79 (2018).
 [17] H. A. Kramers and G. H. Wannier, Statistics of the two-dimensional ferromagnet. Part 1., *Phys. Rev.* **60**, 252 (1941).
 [18] M. T. Tan, Y. Wang, and A. Mitra, Topological defects in floquet circuits, arXiv:2206.06272 (2022).
 [19] E. P. Verlinde, Fusion Rules and Modular Transformations in 2D Conformal Field Theory, *Nucl. Phys. B* **300**, 360 (1988).
 [20] J. L. Cardy, Boundary conditions, fusion rules and the verlinde formula, *Nucl. Phys. B* **324**, 581 (1989).
 [21] V. B. Petkova and J. B. Zuber, Generalized twisted partition functions, *Phys. Lett. B* **504**, 157 (2001).
 [22] J. Fröhlich, J. Fuchs, I. Runkel, and C. Schweigert, Kramers-wannier duality from conformal defects, *Phys. Rev. Lett.* **93**, 070601 (2004).
 [23] C.-M. Chang, Y.-H. Lin, S.-H. Shao, Y. Wang, and X. Yin, Topological Defect Lines and Renormalization Group Flows in Two Dimensions, *J. High Energy Phys.* **01**, 026.
 [24] A. Y. Kitaev, Unpaired majorana fermions in quantum wires, *Phys.-Usp.* **44** (2001).
 [25] P. Fendley, Strong zero modes and eigenstate phase transitions in the xyz/interacting majorana chain, *Journal of Physics A: Mathematical and Theoretical* **49**, 30LT01 (2016).
 [26] M. Thakurathi, A. A. Patel, D. Sen, and A. Dutta, Floquet generation of majorana end modes and topological invariants, *Phys. Rev. B* **88**, 155133 (2013).
 [27] D. J. Yates, F. H. L. Essler, and A. Mitra, Almost strong $(0, \pi)$ edge modes in clean interacting one-dimensional floquet systems, *Phys. Rev. B* **99**, 205419 (2019).
 [28] A. Mitra, H.-C. Yeh, F. Yan, and A. Rosch, Noninte-

- grable floquet ising model with duality twisted boundary conditions, *Phys. Rev. B* **107**, 245416 (2023).
- [29] A. Rahmani, K. J. Sung, H. Putterman, P. Roushan, P. Ghaemi, and Z. Jiang, Creating and manipulating a Laughlin-type $\nu = 1/3$ fractional quantum hall state on a quantum computer with linear depth circuits, *PRX Quantum* **1**, 020309 (2020).
- [30] K. Satzinger et al, Realizing topologically ordered states on a quantum processor, *Science* **374**, 1237 (2021).
- [31] J. P. T. Stenger, N. T. Bronn, D. J. Egger, and D. Pekker, Simulating the dynamics of braiding of Majorana zero modes using an IBM quantum computer, *Phys. Rev. Res.* **3**, 033171 (2021).
- [32] Y.-J. Liu, K. Shtengel, A. Smith, and F. Pollmann, Methods for simulating string-net states and anyons on a digital quantum computer, *PRX Quantum* **3**, 040315 (2022).
- [33] A. Kirmani, K. Bull, C.-Y. Hou, V. Saravanan, S. M. Saeed, Z. Papić, A. Rahmani, and P. Ghaemi, Probing geometric excitations of fractional quantum hall states on quantum computers, *Phys. Rev. Lett.* **129**, 056801 (2022).
- [34] T. I. Andersen et al, Non-abelian braiding of graph vertices in a superconducting processor, *Nature* **618**, 264 (2023).
- [35] N. Harle, O. Shtanko, and R. Movassagh, Observing and braiding topological Majorana modes on programmable quantum simulators, *Nat. Comm.* **14**, 2286 (2023).
- [36] A. Kirmani, D. S. Wang, P. Ghaemi, and A. Rahmani, Braiding fractional quantum hall quasiholes on a superconducting quantum processor, arXiv:2303.04806 (2023).
- [37] X. Mi and et al, Noise-resilient edge modes on a chain of superconducting qubits, *Science* **378**, 785 (2022).
- [38] M. Hauru, G. Evenbly, W. W. Ho, D. Gaiotto, and G. Vidal, Topological conformal defects with tensor networks, *Phys. Rev. B* **94**, 115125 (2016).
- [39] O. Shtanko, D. S. Wang, H. Zhang, N. Harle, A. Seif, R. Movassagh, and Z. Mineev, Uncovering local integrability in quantum many-body dynamics, arXiv:2307.07552 (2023).
- [40] M. B. Hastings and J. Haah, Dynamically Generated Logical Qubits, *Quantum* **5**, 564 (2021).

Supplemental Material for “Generating unpaired Majorana modes in a quantum computer through duality defects”

Sutapa Samanta,¹ Derek S. Wang,² Armin Rahmani,^{1,3} and Aditi Mitra⁴

¹*Department of Physics and Astronomy, Western Washington University, Bellingham, Washington 98225, USA*

²*IBM Quantum, IBM T.J. Watson Research Center, Yorktown Heights, New York 10598, USA*

³*Advanced Materials Science and Engineering Center,*

Western Washington University, Bellingham, Washington 98225, USA

⁴*Center for Quantum Phenomena, Department of Physics,*

New York University, 726 Broadway, New York, New York 10003, USA

In this Supplement, we first discuss numerical evidence for the accuracy of random sampling in estimating the full autocorrelation functions. We then present an analogous graph to Fig. 2 of the main text for the various autocorrelation functions but in the presence of interactions. Finally, we discuss the error mitigation methods employed in improving the quality of the data.

CONVERGENCE OF THE PARTIAL TRACE

In this section, we provide evidence for the accurate approximation of the autocorrelation functions (based on the full trace) by a partial trace with a small number of random basis states. In Fig. 1, we show the expectation value with a single random state, and the partial trace with 20 random initial states, and we compare them with the full trace calculated with all 2^{12} basis states for a system of size $L = 12$. We have calculated these quantities for all three Pauli operators. Even a single expectation value is relatively close to the exact (full trace) autocorrelation function, for both bulk and defect sites, due to the little variation between these expectation values. The results of the partial trace with 20 random states are in excellent agreement with the full trace, supporting the use of the partial trace to approximate the autocorrelation functions. All expectation values are the same for the Y autocorrelation function at the defect sites. Thus for this particular observable, the trace is independent of the number of basis states used.

UNPAIRED MAJORANA IN THE PRESENCE OF INTERACTIONS

In the main text, we discussed the effects of interactions and presented results on the Y autocorrelation function at the defect. In this section, we present more data for other Pauli operators both in the bulk and at the defect, analogous to Fig. 2 of the main text, which was in the absence of interactions. The results exhibit substantial similarities.

ERROR MITIGATION

We employ a composite error mitigation strategy combining error suppression and mitigation techniques [1]. Noisy bitstrings resulting from each shot are first mitigated by correcting readout errors using the method of

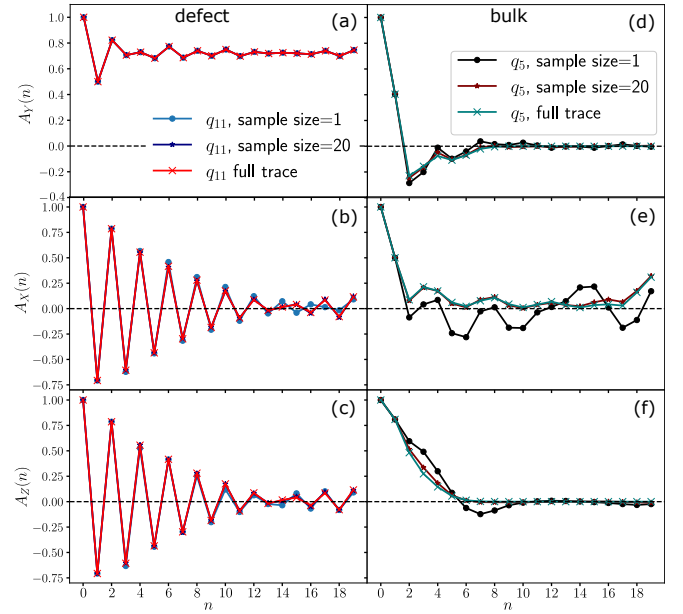


FIG. 1. Autocorrelation functions from computing the partial trace in a classical computer for different sample sizes of random initial states, for system size $L = 12$. The left panels [panel (a), (b), (c)] show the autocorrelation functions at the site of twist defect $r = L - 1$, while the right panels [panel (d), (e), (f)] are for a site far away from it $j = -1 + L/2$.

Ref. 2, which utilizes calibration circuits scaling linearly with the number of qubits. Finally, zero-noise extrapolation is applied by extrapolating measured probabilities to the zero-noise value [3, 4]. This is achieved by performing measurements with 8,000 shots at noise factors of 1 (applying the original circuit) and 3 (evolving the system forward by the original circuit, backward by appending the inverse of the original circuit, and finally forward again by reapplying the original circuit [5]). A line through 1 and 3 on the horizontal axis yield the zero-noise extrapolated value at the intercept with the vertical axis.

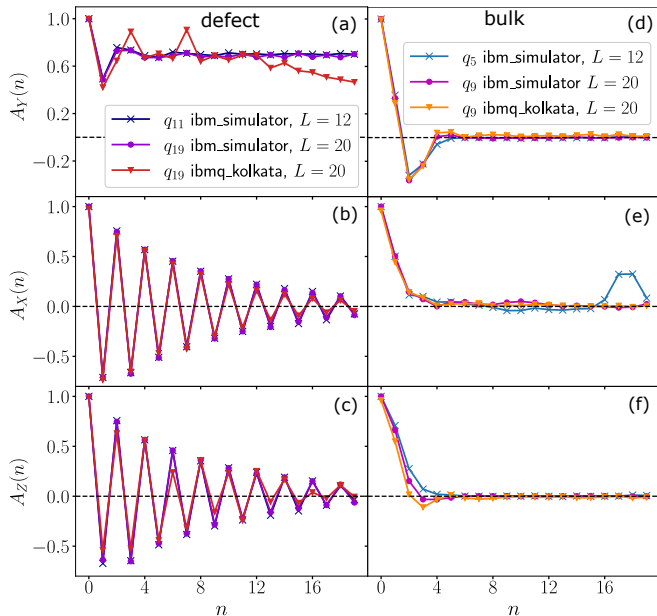


FIG. 2. Signature of Majorana zero mode at the defect site for duality-twisted interacting Floquet-TFIM. Panel (a) shows the non-decaying autocorrelation for σ_y at the defect site $r = L - 1$, which overlaps with the zero mode. All other autocorrelations both at the twist defect $r = L - 1$ [panel (b), (c)] and at a bulk site $j = -1 + L/2$ [panel (d), (e), (f)], far away from the twist defect, decay with time. The chosen bulk qubit behaves qualitatively similarly to other bulk qubits. We present data from `ibmq_kolkata` device for $L = 20$, the longest physical loop of qubits available in the device. There is good qualitative agreement between simulations and measurements on the quantum device. The simulations were also performed for a smaller system of 12 qubits. The agreement between the two system sizes $L = 12, 20$ indicates that we capture the behavior in the thermodynamic limit.

-
- [1] K. J. Ferris, A. J. Rasmuson, N. T. Bronn, and O. Lanes, Quantum simulation on noisy superconducting quantum computers 10.48550/arxiv.2209.02795 (2022).
 - [2] P. D. Nation, H. Kang, N. Sundaresan, and J. M. Gambetta, Scalable mitigation of measurement errors on quantum computers, *PRX Quantum* **2**, 040326 (2021).
 - [3] Y. Li and S. C. Benjamin, Efficient variational quantum simulator incorporating active error minimization, *Phys. Rev. X* **7**, 021050 (2017).
 - [4] K. Temme, S. Bravyi, and J. M. Gambetta, Error mitigation for short-depth quantum circuits, *Phys. Rev. Lett.* **119**, 180509 (2017).
 - [5] P. Rivero, F. Metz, A. Hasan, A. M. Brańczyk, and C. Johnson, Zero noise extrapolation prototype, <https://github.com/qiskit-community/prototype-zne> (2022).